Regular Article

Theoretical Investigation on Inclusion Complex of (s)-2-Isopropyl-1-(o-nitrophenyl) Sulfonyl) Aziridine with β-Cyclodextrin

H. Nouioua[a,b],*, T. Abbaz[a,b], B. Harkati[c], A.K. Gouasmia[a] and D. Villemin[d]

[a]*Laboratory of Organic Materials and Heterochemistry, Larbi Tebessi University, Tebessa, 12000, Algeria*

[b]*Laboratory of Organic Chemistry and Interdisciplinarity "LCOI", University of Mohamed-Cherif Messaadia, Souk Ahras, 41000, Algeria*

[c]*Laboratoryofactive Molecules and Applications, Larbi Tebessi University, Tebessa, 12000, Algeria*

[d]*Laboratory of Molecular and Thio-Organic Chemistry, UMR CNRS 6507, INC3M, FR 3038, Labex EMC3, Ensicaen & University of Caen, Caen 14050, France*

The present work aims to study the theoretical chemistry applied to organic systems such as host/guest inclusion complexes. In literature, different molecular modeling computational methods have been used to study the complexation of the host β-cyclodextrin molecule (β-CD) with the guest (S)-2-Isopropyl-1-(*o*-nitrophenyl) sulfonyl) aziridine molecule (AZ). Among such methods are semi-empirical (PM3) and Density Functional Theory (DFT) calculations in gas and aqueous phases. The present paper focuses on complexation, interaction, deformation energies determination, besides geometries, electronic structure, and chemical reactivity to describe the changes of AZ during encapsulation in two phases and at two orientations. Long-range corrected hybrid functional (WB97X-D/6-31G (d) basis) was used and the results clearly indicate that the formed complex is energetically preferred in both phases. The orientation in which the guest molecule pointed toward the secondary hydroxyls of β-CD showed good compatibility with the experimental results. The Natural Population Analysis (NPA) charges obtained from NBO analysis were used in order to find out the possible coordination modes of the AZ compound with β-CD. Natural bond orbital analysis **(**NBO) and Non-covalent interaction (NCI) analysis were performed on the β-CD/AZ complex to understand the different interactions. The 1H nuclear magnetic resonance (NMR) of the complex was studied using the Gauge-Including Atomic Orbital (GIAO).

Keywords: β-Cyclodextrin, AZ, DFT, NBO and NCI

INTRODUCTION

Cyclodextrins (CDs) are cyclic oligosaccharides that can be obtained artificially by enzymatic conversion of amylose using the enzyme cyclodextrin glycosyltransferase (CGTase) of bacterial origin. The three most commonly used CDs are α-CD, β-CD, and γ-CD, which consist of 6, 7, and 8 subunits of D-glucopyranose, respectively [1,2] linked together by α-glycosidic bonds (1 → 4). Thus the cavity formed has non-polar carbonate and hydrophobic environment, while the outer part contains many hydroxyls

groups, which leads to the solubility of cyclodextrins in an aqueous medium. Due to the presence of mentioned non-polar cavity, cyclodextrins are able to form inclusion complexes in an aqueous medium with a variety of hydrophobic host molecules; the formation of complex depends on a proper match between the size of the host molecule and the cyclodextrin molecule. In this article, β-CD (Fig. 1a) has been used as a host due to its non-toxicity to the human organism. It has been used frequently in the food, pharmaceutical, and cosmetic industries.

Aziridine is an interesting class due to its chemical reactivity. They are valuable natural and/or synthetic organic compounds that are widely used to access many

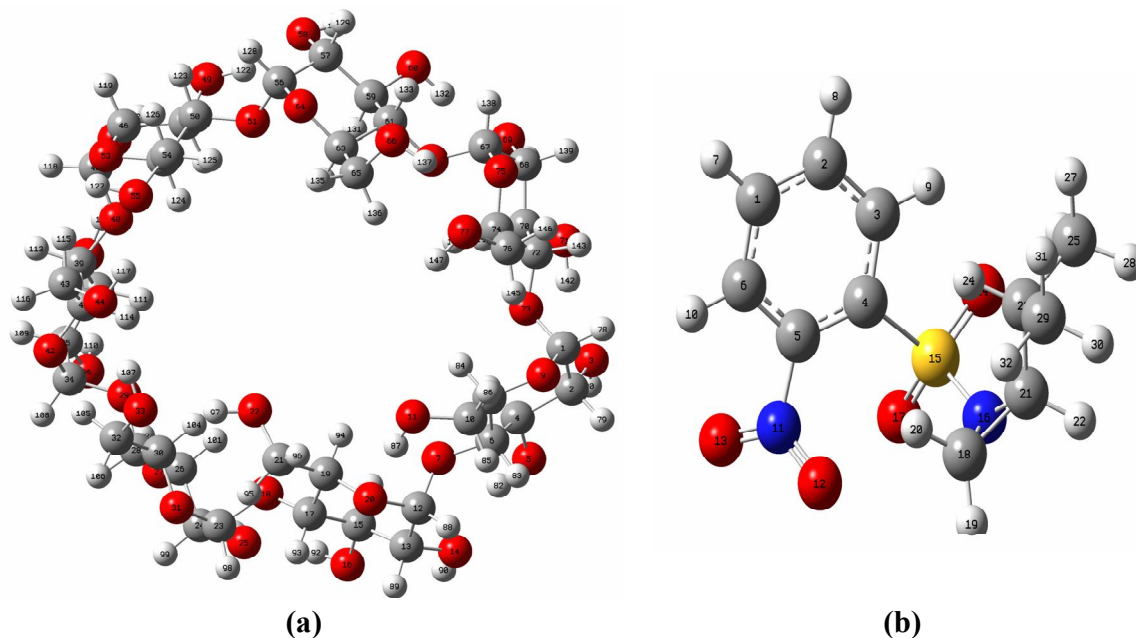*Corresponding author. E-mail: hadjer.nouioua@univ-tebessa.dz

(a)   **(b)**

Fig. 1. Molecular structures and atom numbering for β-CD (a) and AZ (b).

medicines and bioactive products [3,4].

Molecular modeling is a technique that not only can represent the chemical properties and chemical reactions, but also to manipulate the structure of model compounds in two or three dimensions. Actually, there are a large number of theoretical methods used in the molecular modeling of supramolecular systems. Among these methods are molecular mechanics (MM), molecular dynamics (MD), semi-empirical methods, and DFT methods that are widely used for large systems to determine the graphical representation of the geometry or configuration of the atoms of a molecule and assessing the physical and chemical properties of the molecule. Molecular modeling associated to a graphical representation of the stereochemistry allows interpretation of physical and chemical phenomenon, suggesting new experiments, and thus analyzing the results in a more significant way than the traditionally used experiments. In fact, both approaches, pure theoretical and experiment, are complementary.

This work is composed of two parts: in the first part, the processes of AZ inclusion in the β-CD cavity are examined using the semi-empirical PM3 method for determining minimum energy structures. In the second part, the more stable complex, obtained through PM3 calculations, are improved by the density functional theory (DFT) using the functionals B3LYP [5,6], WB97X-D [7], and B97D3 [8,9], and 6-31G(d) basis set in gas and aqueous phases. In this part, complexation, interaction, and deformation energies, geometries, thermodynamic parameters, frontier molecular orbitals, the global indices of reactivity, the (NPA) atomic charges, and natural bond orbital (NBO) are calculated. We also systematically compare the chemical shifts deviations obtained from Gauge-Including Atomic Orbital calculations (GIAO) and corresponding experimental values of 1H NMR [10].

Finally, analysis of non-covalent interactions (NCI) as a robust approach for evaluating intermolecular interactions is considered.

COMPUTATIONAL DETAILS

Quantum mechanical calculations were performed using density functional theory (DFT) applying the functionals B3LYP [5,6], WB97X-D [7], and B97D3 [8,9], and the 6-31G(d) basis set in the gas and aqueous phases. Gaussian 09 [11] and MOPAC 2016 [12] software were used.
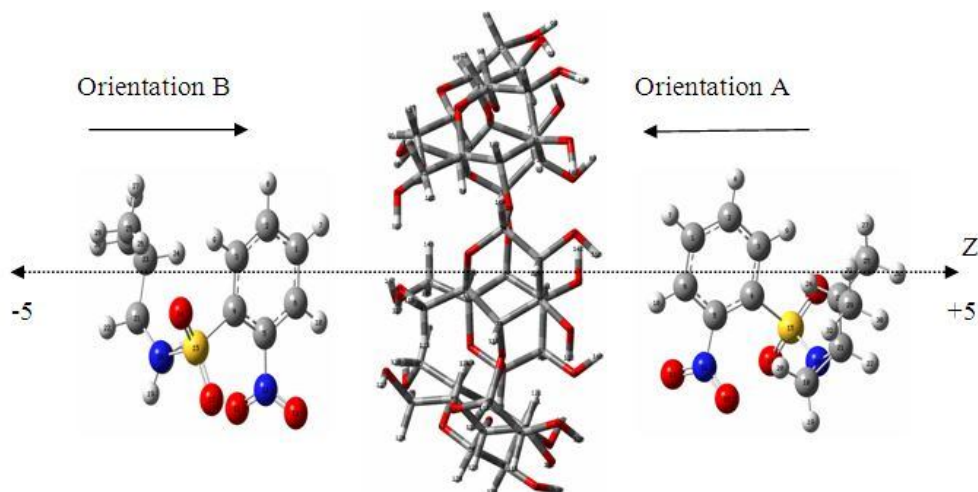
Fig. 2. Coordinate systems used to define the complexation process for both orientations.

The initial structures of the guest AZ and the host β-CD were retrieved from PUBCHEM compound database [13] and Chem office3D Ultra (version10, Cambridge Software) [14], respectively The AZ/β-CD complex was generated by Hyperchem 7.5 [15] molecular modeling software. The AZ and β-CD structures were optimized by the semi-empirical PM3 method [16]. Semi-empirical calculations were first performed using MOPAC 2016 [12], and the visualization and treatment of results were done using Gauss view 5.0 [17]. The optimized host and guest structures are shown in Fig. 1.

The coordinate system used to define complexation process is shown in Fig. 2. To inclusion the guest AZ molecule inside the β-CD, methods described in the literature have been followed [18-22]. The β-CD host is positioned at the XY plane and its center is defined as the origin of the systems coordinates. The secondary hydroxyl groups of β-CD are oriented in the positive direction of the Z axis, and then the mass center of the guest molecule AZ is placed at the XYZ reference center. The center of the β-CD host is located at the origin of the reference frame, O (0, 0.0) and β-CD is in fixed position. The guest to host is then moved along the Z axis from -5 to +5 A0 with 1 Å step. Figure 2 shows two directions for insertion of guest molecule into the β-CD host molecule. This allows us to see the effects of the two types of hydroxyls: Orientation A, in which the aromatic ring is oriented toward the secondary hydroxyls of β-CD, and Orientation B, in which the

aromatic ring is oriented towards the basic hydroxyls of β-CD.

To define the host-guest interaction in the optimized geometries, several energetic expressions were used: complexation energy [23], interaction energy [24,25], and deformation energy [26].

The complexation energy is defined as the difference between the energy of the complex and the energy of the individual components in their optimized geometries, Eq. (1).

$$\Delta E_{complexation} = E_{complex} - [E_{\beta-CDfree} + E_{AZ\,free}] \qquad (1)$$

Where $E_{complex}$ represents the energy of the complex, $E_{\beta-CD}$ represents the energy of β-CD before the complexation, and E_{AZ} represents the energy of the AZ guest molecule before the complexation.

Interaction energy represents the interaction between host molecule and the guest molecule in the inclusion complex (Eq. (2)).

$$\Delta E_{interaction} = E_{complex} - [E_{\beta-CDsp} + E_{AZsp}] \qquad (2)$$

Where $E_{complex}$ represents the energy of the complex, $E_{\beta-CD}$ represents the energy of β-CD after the complexation, and E_{AZ} represents the energy of the guest molecule after the complexation.

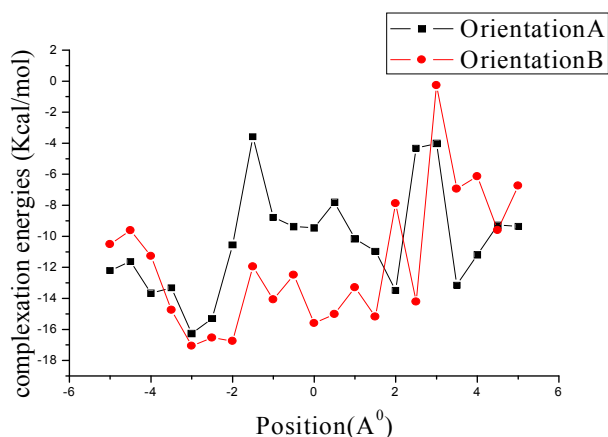The last energy is the deformation energy of each host

71

Fig. 3. Complexation energies of the inclusion of AZ into β-CD optimized at different positions Z using (PM3 calculations).

and guest component during the formation of the complex. It is defined as the difference between the energy of the fully optimized component compared to its energy in the complex (Eqs. (3) and (4)).

$$E_{deformation\ (\beta\text{-}CD)} = E_{\beta\text{-}CD\ sp} - E_{\beta\text{-}CD\ free} \tag{3}$$

$$E_{deformation\ (AZ)} = E_{AZ\ sp} - E_{AZ\ free} \tag{4}$$

RESULTS AND DISCUSSIONS

Energies

The graphical presentation of the energy changes for the insertion of AZ in the β-CD are shown as two curves in Fig. 3. From these curves, it is observed that the minimum energy of the more stable structures falls at Z = -3 Å, and Z = -3 Å for the two orientations A and B, respectively. The corresponding complexation energies are: -16.260 kcal mol^{-1} and -17.063 kcal mol^{-1} for orientations A and B, respectively. After that, the resulting complex was optimized at a high computational level using the following functionals: B3LYP/6-31G(d) and WB97X- D/6-31G(d) and B97D3/6-31G(d)) in gas and aqueous phases. The calculation of the different energy conditions for the two orientations were reported and compared in Table 1. From Table 1, it is observed that, in contrast to PM3 semi-empirical calculations, the interaction energy is in favor of

Table 1. The Different Energies of β-CD/AZ in the Gas and Aqueous Phase were Calculated by Methods: B3LYP/6-31G(d), WB97X-D/6-31G(d), and B97D3/6-31G(d)

|	Gas phase		Aqueous phase	
	Orientation A	Orientation B	Orientation A	Orientation B
B3LYP/6-31G(d)				
$\Delta E_{complexation}$	-19.60	-6.80	-11.37	-3.52
$\Delta E_{interaction}$	-25.58 (-12.01)	-8.74 (0.31)	-14.82	-4.42
$E_{DEF(Host)}$	9.52	1.38	5.79	0.53
$E_{DEF(Guest)}$	-3.54	0.56	-2.34	0.36
WB97X-D/6-31G(d)				
$\Delta E_{complexation}$	-41.06	-37.02	-31.85	-31.38
$\Delta E_{interaction}$	-52.35 (-39.24)	-46.56 (-32.00)	-40.37	-38.67
$E_{DEF(Host)}$	12.84	6.74	9.05	4.53
$E_{DEF(Guest)}$	-1.53	2.80	-0.52	2.75
B97D3/6-31G(d)				
$\Delta E_{complexation}$	-41.66	-37.85	-33.41	-33.89
$\Delta E_{interaction}$	-52.15 (-36.65)	-47.22 (-30.38)	-40.86	-39.77
$E_{DEF(Host)}$	12.20	6.66	8.17	3.77
$E_{DEF(Guest)}$	-1.70	2.70	-0.71	2.10
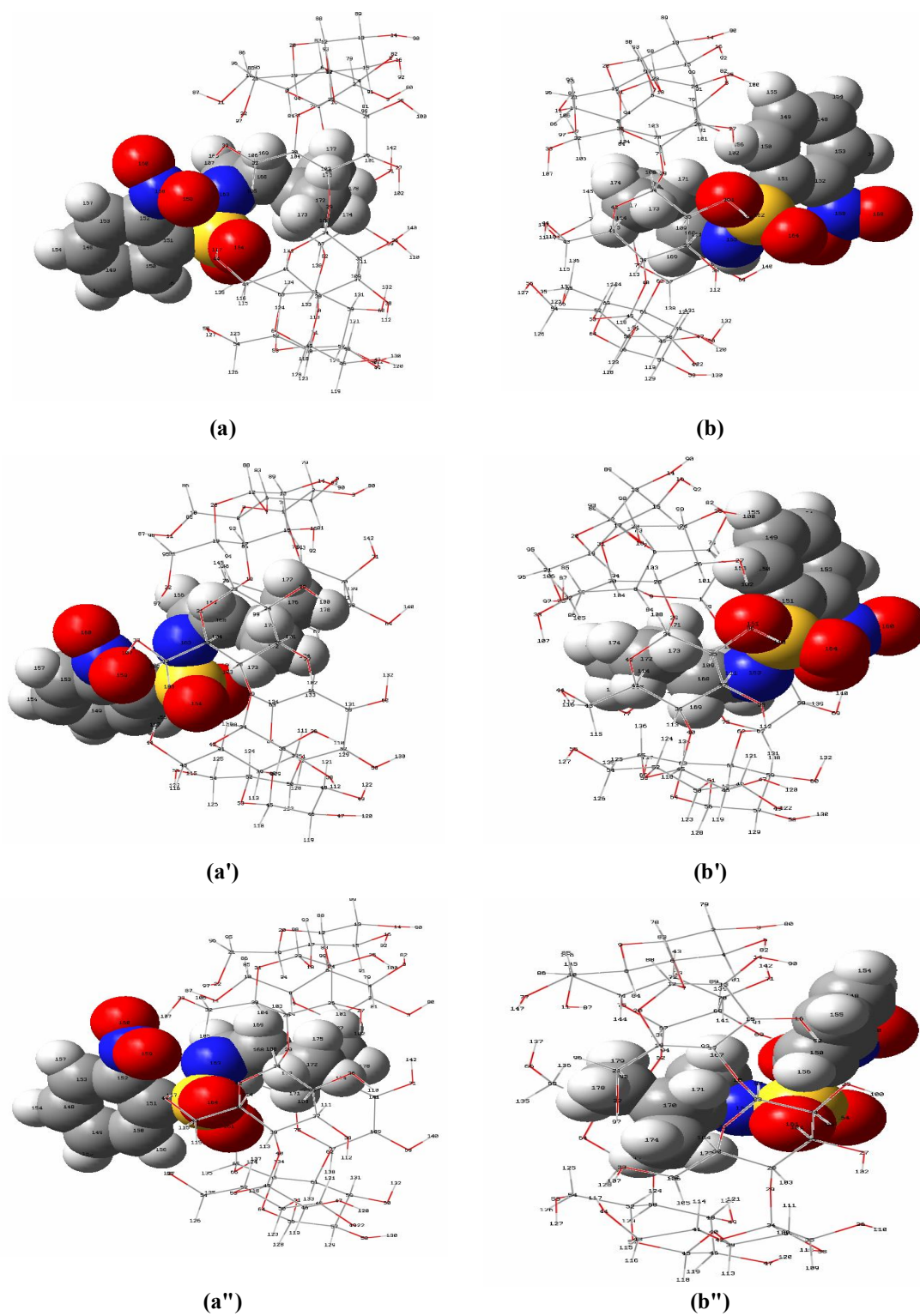
Fig. 4. Geometrical structures of the most stable complexes obtained from B3LYP/6-31G(d) (a, b), WB97X-D/6-31G(d) (a', b') and B97D3/6-31G(d) (a'', b'') calculations for AZ/β-CD in gas phase.
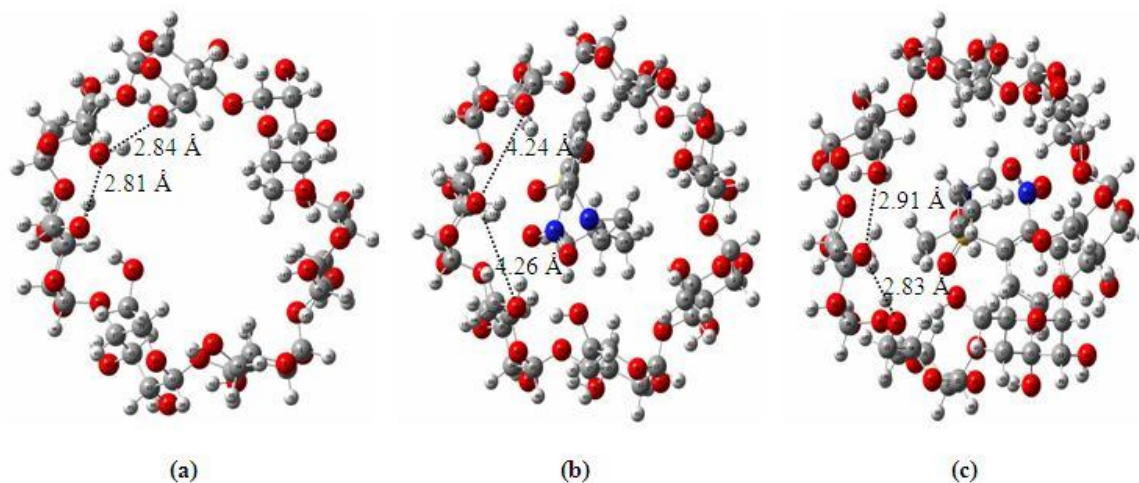
Fig. 5. Geometric structures of the free β-CD (a) and the AZ/β-CD complex (b, c) in the orientations A and B calculated by the method WB97X-D/6-31G(d) in the gas phase.

orientation A. It is worth noting that the complexation and interaction energies have negative values, indicating that the inclusion of AZ in β-CD is thermodynamically favorable, and the encapsulation processes and the calculations are in good agreement with experimental data [10]. Significantly higher values of $\Delta E_{interaction}$ energy obtained using WB97X-D/6-31G(d) (-52.35 kcal mol^{-1}) and B97D3/6-31G(d) (-40.86 kcal mol^{-1}) methods, compared to B3LYP/6-31G(d) (-25.58 kcal mol^{-1}) method. For the two methods, WB97X-D/6-31G(d) and B97D3/6-31G(d), the dispersion effect is an important factor to study the supramolecular systems; weak dispersion forces increase with increasing the number of atoms and the molecular weight [19]. The effects of electron correlation play an important role on the nature of intermolecular interaction probably having a considerable contribution to dispersion forces [19]. The solvent effect is indicated by energy difference between the gas and aqueous phases. The results of the deformation energies of the gas and aqueous phases calculated by the three functionals are shown in Table 1. From the results, the deformation energy of the β-CD molecule is always higher than that of the AZ molecule in both orientations, A and B. This confirms that the flexibility of the β-CD structure plays an important role in increasing the intermolecular interaction and affects the stability of the whole system upon complexation [25]. Especially, the primary hydroxyl groups of β-CD play an important role in the formation of bonds with AZ

(see Fig. 5).

We also note that the deformation energy of the β-CD molecule calculated by the classic B3LYP method (9.52 kcal mol^{-1}) is lower than that obtained using the WB97X-D/6-31G(d) (12.84 kcal mol^{-1}) and B97D3/6-31G(d) (12.20 kcal mol^{-1}) methods. This indicates that WB97X-D/6-31G(d) and B97D3/6-31G(d) predict better optimized geometries than the traditional B3LYP method.

To improve the accuracy of our theoretical results, from the computation of optimized geometries, the interaction energy was corrected considering the basic set superposition error (BSSE) [27] using the counterpoise method [28] through (Eq. (5)).

$$\Delta E_{interaction} = E_{complex} - [E_{\beta-CDsp} + E_{AZsp}] + BSSE \qquad (5)$$

BSSE corrected energies are shown in brackets in Table 1.

Geometry Optimization

According to our results, most of the geometric parameters have approximately the same values in both the gas state and the aqueous state. This let us to provide a single interpretation in the gas axis. Tables 2 and 3 report the geometrical parameters (bond lengths, bond angles, and dihedral angles) of the AZ and β-CD molecules before and after complexation, which are related to the most stable

74

Table 2. Geometric Parameters (Bond Lengths, Bond Angles and Dihedral Angles) for AZ before and after Inclusion in β-CD Calculated with B3LYP/6-31G(d)/WB97X-D/6-31G(d)/B97D3/6-31G(d) in the Gas Phase

	Gas phase		
	AZ free	Orientation A	Orientation B
Bond lengths (Å)			
O 164–O 161	2.54/2.52/2.56	2.52/2.49/2.53	2.53/2.51/2.54
O 164–S 162	1.45/1.44/1.46	1.47/1.45/1.47	1.45/1.44/1.46
S 162–O 161	1.46/1.45/1.47	1.47/1.45/1.48	1.47/1.45/1.47
N 163–C 165	1.45/1.45/1.46	1.48/1.47/1.48	1.46/1.45/1.47
Bond angles (°)			
S 162–O 164–C 151	42.10/41.96/41.92	38.89/38.00/37.84	42.04/42.35/42.02
S 162–O 164–O 161	29.75/29.49/29.39	31.01/31.28/31.04	30.32/30.23/30.24
S 162–N 163–O 164	33.20/33.32/33.54	33.15/33.34/33.50	33.18/33.22/33.43
S 162–N 163–O 161	34.01/34.20/33.87	30.83/30.68/30.16	33.24/33.16/32.53
N 158–O 159-O 160	27.31/27.18/27.00	27.39/27.26/27.07	27.33/27.44/27.34
Dihedral angles (°)			
S 162–O 164–O 161–C 151	-41.76/-41.48/-41.14	-37.48/-36.13/-35.81	-41.61/-41.63/-41.15
S 162–O 164–O 161–N 163	38.81/38.50/39.41	32.49/32.32/32.13	37.82/36.89/37.30
S 162–N 163–O 164–O 161	29.42/29.12/29.08	26.27/26.35/25.65	29.16/28.66/28.37
S 162–N 163–O 161–C 151	39.31/39.86/39.14	46.47/47.45/47.97	39.45/39.85/39.74
N 158–O 159–O 160–C 152	-2.04/-2.42/-2.46	2.37/2.57/2.76	-2.09/-1.40/-1.40

Table 3. The Selected Parameters for Free β-CD and In-complex Forms Calculated with B3LYP/6-31G(d)/WB97X-D/6-31G(d)/B97D3/6-31G(d) Methods in the Gas Phase

	Gas phase		
	β-CD free	Orientation A	Orientation B
Primary hydroxyls			
O 33–O 44	2.90/2.83/2.85	4.37/4.21/4.32	2.91/2.85/2.92
O 44–O 55	2.91/2.84/2.86	4.48/4.16/4.26	2.94/2.92/3.09
O 55–O 66	6.64/6.45/6.52	6.56/6.21/6.30	6.74/6.71/6.91
O 66–O 77	3.00/2.94/2.96	3.25/3.22/3.16	3.00/2.91/2.97
Secondary hydroxyls			
O 71–O 60	5.61/5.60/5.63	5.56/5.54/5.60	5.68/5.66/5.69
O 60–O 49	5.27/5.22/5.23	5.31/5.36/5.36	5.27/5.23/5.20
O 49–O 38	5.50/5.44/5.49	5.18/5.22/5.19	5.51/5.37/5.35
O 38–O 27	5.65/5.57/5.65	5.32/5.29/5.31	5.61/5.37/5.53

structures obtained with B3LYP/6-317G(d), WB97X-D/6-31G(d), and B97D3/6-31G(d) methods. As shown in Table 2, the results for the orientation A indicate that the initial geometry of guest AZ is completely changed. This is while the difference in the geometric parameters before and after the complexation slightly changed for the orientation B. Initially, there was a slight change observed in the bond lengths of the AZ before (O 164-S 162: 1.45/1.44/1.46 Å) and after the complexation in the orientation A (O 164-S 162: 1.47/1.45/1.47 Å) and in the orientation B (O 164-S 162: 1.45/1.44/1.46 Å). The real change was observed through the difference between the bond angles and dihedral angles of the AZ molecule before and after the complexation. For orientation A, the difference between the S 162-O 164-O 161-N 163 dihedral angle (38.810/38.50°/ 39.41°) of the free AZ molecule and the dihedral angle S 162-O 164-O 161-N 163 (32.49°/32.32°)/32.13°) of AZ in the complex is important. The mentioned difference is more obvious compared to the similar results of dihedral angle S 162-O 164-O 161-N 163 (37.820/36.890/37.30°) in the orientation B. This means that the guest AZ in the orientation A must be profiled to fit the host β-CD cavity and form a more stable inclusion complex. This result was confirmed by deformation energies (see Table 1). On the other hand, the distances between the primary and secondary hydroxyls' oxygens of β-CD and AZ, before and after complexation, (Table 3) show significant distortion in the β-CD lumen compared to its initial geometry (see Fig. 5). In the orientation A, the O 33-O 44 (2.83 Å) and O 44-O 55 (2.84 Å) distances became longer (4.21 Å and 4.16 Å, respectively), which is due to interactions between O164 and H 117 from oxygen O44 and between O 159 and H 107 oxygen O 33; the latter is present in the orientation A, but not in the orientation B (see Fig. 5). This explains why the interaction energy of inclusion in the orientation A (-52.35 kcal mol^{-1}) is less than that in the orientation B (-46.56 kcal mol^{-1}) in both phases using all three functionals.

Thermodynamic Properties

Calculations of standard thermodynamic parameters were performed using harmonic vibrational analysis [29]. Calculations were performed in vacuum and water at 1 atm pressure and temperature of 298.15 K using WB97X-D/6-31G(d), and B97D3/6-31G(d) methods. The thermodynamic quantities of the AZ/β-CD complex, such as the enthalpy change (ΔH°), the thermal Gibbs free energy (ΔG°), and entropy contribution (ΔS°) are summarized in Table 4.

It was observed that the enthalpy values (ΔH°) are negative in both orientations, and these differences indicate that the inclusion process is enthalpically favorable. On the other hand, the enthalpy differences of the orientation A (ΔH° = -48.67 kcal mol^{-1}) were more negative than that in orientation B (ΔH° = -42.89 kcal mol^{-1}), which is attributed to stronger van der Waals interactions [25] between AZ and β-CD in deeper penetration of the guest molecule into the hydrophobic host. Values of ΔG° = -60.01 cal mol^{-1} K^{-1} are negative and this indicates that the process of AZ inclusion in β-CD is spontaneous at 1 atm and 298.15 K. when the system is well arranged, the results of our theoretical calculations ΔG° < 0 is in good agreements with the data in the literature [10]. We can also see that the entropy (ΔS°) has a negative change in both orientations. This indicates that the formation of the complex is an exothermic process resulting from enthalpy [20]. Due to steric barrier, the negative change of the entropy (ΔS°) caused by molecular geometrical shape that limits the free shift of β-CD cavity and rotation of AZ molecule [20].

Frontier Molecular Orbitals (FMOs)

The occupied HOMO and unoccupied LUMO frontier molecular orbitals [30] play an important role in understanding the effect of guest molecule encapsulation within the host. HOMO is the electron donor and LUMO is the electron acceptor [31,32]. Results for the energies of HOMO and LUMO, and ΔE (HOMO-LUMO) obtained by WB97X-D/6-31G(d) and B97D3/6-31G(d) methods in the gas and aqueous phases are shown in Table 4. The energy gap ΔE (HOMO-LUMO) is an important measure of stability. The higher chemical values of ΔE (HOMO-LUMO) indicate higher stability and lower reactivity [33-35]. The values of ΔE (HOMO-LUMO) obtained by the two methods in the gas and aqueous phases of the AZ/β-CD complex are -0.291 eV for orientation A and -0.297 eV for orientation B. This means that orientation A is more stable than orientation B. These results are in good agreement with the complexation energy results of the orientation A (41.66 kcal mol^{-1}) and the orientation

Table 4. Thermodynamic Parameters, HOMO, LUMO, Δ(HOMO-LUMO) and Global Descriptions of the AZ, β-CD, and AZ/β-CD Complex Computed by Methods WB97X-D/6-31G(d)/ B97D3/6-31G(d)) in the Gas and Aqueous Phases

Gas phase				
	β-CD free	AZ free	Orientation A	Orientation B
ΔH° (kcal mol^{-1})	-	-	-48.67/-48.35	-42.89/-44.71
ΔG° (kcal mol^{-1})	-	-	-30.70/-32.97	-24.80/-26.43
ΔS° (cal mol^{-1} K^{-1})	-	-	-60.01/-52.81	-60.54/-59.04
HOMO	-0.32/-0.19	-0.35/-0.22	-0.32/-0.19	-0.33/-0.20
LUMO	0.11/0.01	-0.02/-0.11	-0.02/-0.12	-0.03/-0.13
ΔE (HOMO-LUMO)	-0.44/-0.20	-0.32/-0.11	-0.291/-0.06	-0.297/-0.07
μ (eV)	-0.10/-0.09	-0.1868/-0.174	-0.175/-0.16	-0.1862/-0.171
x (eV)	0.10/0.09	0.1868/0.174	0.175/0.16	0.1862/0.171
η (eV)	0.22/0.10	0.16/0.05	0.145/0.032	0.148/0.036
ω (eV)	0.02/0.04	0.106/0.27	0.105/0.39	0.11/0.40

Aqueous phase				
	β-CD free	AZ free	Orientation A	Orientation B
ΔH° (kcal mol^{-1})	-	-	-37.05/-39.25	-34.91/-36.29
ΔG° (kcal mol^{-1})	-	-	-21.60/-18.84	-19.65/-16.76
ΔS° (cal mol^{-1} K^{-1})	-	-	-51.64/-66.23	-50.95/-65.52
HOMO	-0.33/-0.20	-0.35/-0.23	-0.33/-0.20	-0.33/-0.20
LUMO	0.12/0.01	-0.02/-0.12	-0.03/-0.13	-0.04/-0.13
Δ(HOMO-LUMO)	-0.46/-0.22	-0.32/-0.10	-0.295/-0.06	-0.290/-0.07
μ (eV)	-0.10/-0.09	-0.19/-0.180	-0.182/-0.168	-0.188/-0.171
x (eV)	0.10/0.09	0.19/0.180	0.182/0.168	0.188/0.171
η (eV)	0.23/0.11	0.16/0.05	0.147/0.033	0.145/0.036
ω (eV)	0.02/0.03	0.111/0.29	0.113/0.41	0.12/0.43

B (-37.85 kcal mol^{-1}). The Frontier orbitals of AZ/β-CD in the two obtained phases were calculated by B97D3/6-31G(d). Results indicate that HOMO orbit is localized on the host, and the LUMO orbit is localized on the guest molecule, which means mutual interactions are generated between β-CD and AZ (see Fig. 6).

The Global Indices

The energy gap between HOMO and LUMO can be used in determining the global indices of the reactivity such as electronegativity (χ), electronic potential (μ), hardness (η), and global electrophilicity index (ω). Indices of the reactivity were calculated by the methods WB97X-D/6-

31G(d) and B97D3/6-31G(d) in gas and aqueous phases using the following equations:

$$\mu = (E_{HOMO} + E_{LUMO})/2 \tag{6}$$

$$\chi = -\mu = (E_{HOMO} + E_{LUMO})/2 \tag{7}$$

$$\eta = (E_{LUMO} - E_{HOMO})/2 \tag{8}$$

$$\omega = \mu^2/2\eta \tag{9}$$

Table 4 shows the global indices of reactivity. It is clear that the values of the electronic potential (μ) are negative in the
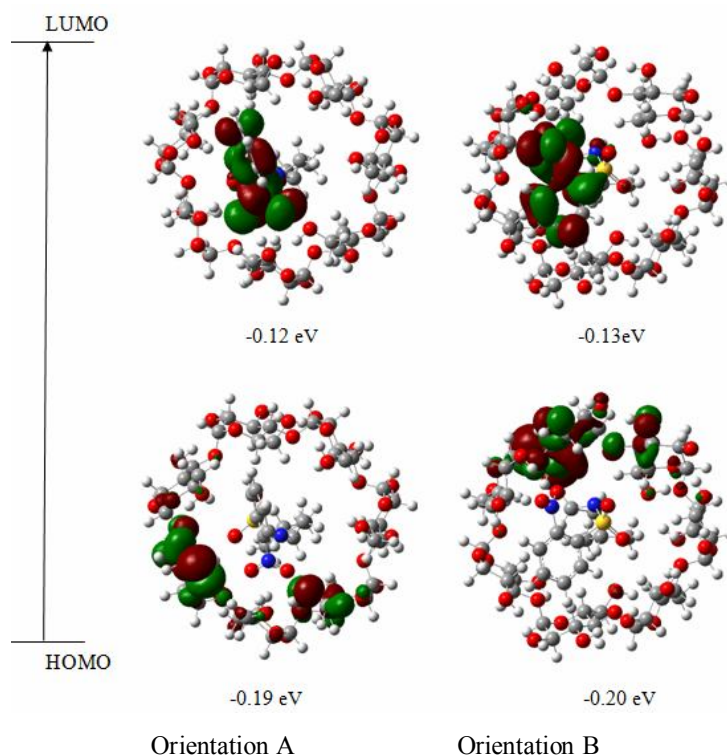
Fig. 6. The Frontier orbitals HOMO and LUMO of the AZ/β-CD complex was obtained using the B97D3/6-31G(d) method in the gas phase.

two phases, and the two orientations. This demonstrates that the complexation of the AZ in the β-CD cavity is a spontaneous phenomenon. Using WB97X-D/6-31G(d) method in the gas and aqueous phases, the electronic chemical potential of the free AZ molecule was less than that of the free β-CD. This difference allows the charge transfer from the β-CD, with high electronic chemical potential (-0.10/-0.10 eV), to AZ, with low electronic chemical potential (-0.18/-019 eV) [36]. From the values in the Table 4, it is clear that the chemical hardness of AZ/β-CD is important in both orientations, confirming the charge transfer. From the results obtained for the total global electrophilicity index, we can conclude that the compound is electrophilic.

Atomic Charges

The charge distribution in the AZ/β-CD complex was analyzed using two population analysis methods: The Mulliken Population Analysis (MPA), and NPA; our goal was to compare them and assess their utility. Mulliken

atomic charge analysis was performed to identify the partial atomic charges that o allow the qualitative understanding of the structures and reactivity of molecules. The charge distributions of atoms calculated by the NBO approach are presented in Table 5. WB97X-D/6-31G(d) and B97D3/6-31G(d) methods were used to study the free and encapsulated AZ in the gas phase and in different orientations. From these results, it can be seen that all the atomic charges of AZ were altered upon complexation with the host β-CD. The results showed that the positive charges were localized on hydrogen (H 171: 0.177/0.164) and sulfur atoms (S 162: 1.361/1.285). The negative charges were localized on oxygen (O 160: -0.356/-0.331) and carbon atoms (C 170: -0.155/-0.128). Nitrogen atoms can be either positive (N 158: 0.405/0.360), due to the presence of high electronegative oxygen atoms (O 159: -0.396/-0.368 and O 160: -0.356/-0.331) in the adjacent position, or negative (N 163: -0.577/-0.540), due to the attachment of the positively charged sulfur atom (S 162: 1.361/1.285). We can also see that in both orientations, the H atoms (H 166,

Table 5. Variation of Mulliken Atomic Charges of AZ before and after Inclusion into β-CD Calculated by WB97X-D/6-31G(d) and B97D3/6-31G(d) in the Gas Phase

N° = Atome	AZ free	Orientation A	Orientation B
C 148	-0.173/-0.142	-0.174/-0.141	-0.162/-0.130
C 149	-0.144/-0.111	-0.144/-0.111	-0.147/-0.126
C 150	-0.188/-0.172	-0.138/-0.139	-0.191/-0.189
C 151	-0.221/-0.194	-0.193/-0.173	-0.229/-0.205
C 152	0.239/0.239	0.251/0.254	0.249/0.259
C 153	-0.154/-0.122	-0.153/-0.122	-0.166/-0.137
H 154	0.200/0.164	0.199/0.165	0.203/0.169
H 155	0.198/0.162	0.200/0.166	0.191/0.171
H 156	0.234/0.203	0.221/0.208	0.236/0.219
H 157	0.223/0.184	0.220/0.183	0.228/0.196
N 158	0.396/0.352	0.405/0.360	0.414/0.365
O 159	-0.373/-0.344	-0.396/-0.368	-0.405/-0.379
O 160	-0.367/-0.340	-0.356/-0.331	-0.352/-0.330
O 161	-0.546/-0.508	-0.564/-0.531	-0.548/-0.512
S 162	1.300/1.211	1.361/1.285	1.298/1.213
N 163	-0.514/-0.482	-0.577/-0.540	-0.524/-0.493
O 164	-0.512/-0.476	-0.561/-0.530	-0.513/-0.478
C 165	-0.225/-0.205	-0.275/-0.270	-0.250/-0.263
H 166	0.212/0.187	0.233/0.211	0.224/0.230
H 167	0.191/0.178	0.216/0.213	0.182/0.174
C 168	-0.001/0.009	-0.029/-0.02	-0.007/-0.013
H 169	0.194/0.169	0.248/0.234	0.191/0.187
C 170	-0.145/-0.116	-0.155/-0.128	-0.129/-0.105
H 171	0.145/0.135	0.177/0.164	0.153/0.145
C 172	-0.515/-0.478	-0.521/-0.504	-0.531/-0.536
H 173	0.213/0.201	0.201/0.199	0.201/0.197
H 174	0.160/0.143	0.162/0.145	0.191/0.184
H 175	0.163/0.147	0.172/0.167	0.134/0.141
C 176	-0.494/-0.456	-0.522/-0.505	-0.513/-0.493
H 177	0.166/0.152	0.175/0.170	0.149/0.135
H 178	0.171/0.154	0.168/0.151	0.220/0.209
H 179	0.168/0.152	0.173/0.174	0.154/0.151
Charge transfer	0.000/-0,004	0.036/0.056	-0.049/-0.045

H 167, H 171, H 174) of AZ interact with the internal part of β-CD increasing their atomic charges. A significant change in trend was obtained in orientation A: C 168 (-0.001/0.009-0.029/-0.02). The data shows that the charge

Table 6. Calculated Net Charges by Mulliken Population Method and Natural Population Analysis (NPA) of the AZ/β-CD Complex by WB97X-D/6-31G(d) in the Gas Phase

	Orientation A		Orientation B	
N° = Atome	Mulliken charges	NPA	Mulliken charges	NPA
C 148	-0.174	-0.210	-0.162	-0.211
C 149	-0.144	-0.212	-0.147	-0.218
C 150	-0.138	-0.175	-0.191	-0.216
C 151	-0.193	-0.307	-0.229	-0.329
C 152	0.251	0.088	0.249	0.077
C 153	-0.153	-0.223	-0.166	-0.218
H 154	0.199	0.260	0.203	0.266
H 155	0.200	0.261	0.191	0.255
H 156	0.221	0.278	0.236	0.287
H 157	0.220	0.275	0.228	0.281
N 158	0.405	0.560	0.414	0.560
O 159	-0.396	-0.405	-0.405	-0.417
O 160	-0.356	-0.345	-0.352	-0.341
O 161	-0.564	-0.978	-0.548	-0.973
S 162	1.361	2.405	1.298	2.403
N 163	-0.577	-0.761	-0.524	-0.735
O 164	-0.561	-0.964	-0.513	-0.931
C 165	-0.275	-0.268	-0.250	-0.261
H 166	0.233	0.271	0.224	0.257
H 167	0.216	0.240	0.182	0.226
C 168	-0.029	-0.065	-0.007	-0.055
H 169	0.248	0.283	0.191	0.251
C 170	-0.155	-0.293	-0.129	-0.281
H 171	0.177	0.260	0.153	0.249
C 172	-0.521	-0.698	-0.531	-0.696
H 173	0.201	0.251	0.201	0.253
H 174	0.162	0.240	0.191	0.249
H 175	0.172	0.233	0.134	0.207
C 176	-0.522	-0.694	-0.513	-0.692
H 177	0.175	0.234	0.149	0.223
H 178	0.168	0.244	0.220	0.272
H 179	0.173	0.236	0.154	0.228

transfer in the orientation A (0.036) is greater than in the orientation B (-0.049), so the AZ/β-CD complex is more stable in the orientation A than in the orientation B [37]. A method of natural population analysis has been developed to calculate atomic charges and orbital populations of molecular wave functions in general atomic orbital basis sets [38]. For the AZ/β-CD complex, the net charges are calculated by Natural Population Analysis (NPA). The calculated natural atomic charge values were obtained from the Natural Bond Orbital Analysis (NBO) [39] and are listed in Table 6. The natural population analysis is an alternative to conventional Mulliken population analysis, and seems to exhibit improved numerical stability to better describe the electron distributions in AZ/β-CD complex.

Table 7. Stabilization Energy $E^{(2)}$ (kcal mol^{-1}) of the most Important Donor-acceptor Interactions Calculated by WB97X-D/6-31G(d) and B97D3/6-31G(d) in the Two Phases for the Two Orientations

Orbital donor	Orbital acceptor	$E^{(2)}$ (kcal mol^{-1}) WB97X-D/B97D3 Gas phase	$E_{(2)}$ (kcal mol^{-1}) WB97X-D/B97D3 Aqueous phase	d (Å)
Orientation A				
σ(1) (O 161-S 162)	σ*(1) (C 63-H 134)	0.61/0.47	0.61/0.36	2.34
LP(2) (O 11)	σ*(1) (C 165-H 166)	3.76/2.37	4.12/2.01	2.30
LP(1) (O 159)	σ*(1) (O 44-H 117)	3.01/1.48	2.87/1.64	2.19
LP(2) (O 159)	σ*(1) (O 33-H 107)	12.06/10.62	13.84/11.73	1.87
LP(1) (O 164)	σ*(1) (O 44-H 117)	4.89/3.43	5.33/3.44	2.02
Total		24.33/18.37	26.77/19.18	-
Orientation B				
LP(2) (O 16)	σ*(1) (C 149-H 155)	1.25/0.79	1.17/0.81	2.57
LP(1) (O 62)	σ*(1) (O 165-H 166)	5.1/4.56	4.81/2.7	2.16
LP(1) (O 159)	σ*(1) (O 69-H 140)	5.53/4.31	5.98/4.09	1.91
LP(2) (O 159)	σ*(1) (O 69-H 140)	6.68/6.21	6.41/4.64	1.91
Total		18.56/15.87	18.37/12.24	-

Natural Bond Orbital Analysis (NBO)

In order to determine intra- and intermolecular bounds and interactions [40] between guest AZ and host β-CD, to identify, and quantify the different donor-acceptor interactions of the host/guest partners, we used the energy $E^{(2)}$ in Eq. (10); if $E^{(2)}$ is larger, the interactions between donors and acceptor is intense [41]. The delocalization of the electron density between occupied orbitals and unoccupied orbitals is related to the stabilizing donor-acceptor interaction [42].

$$E^{(2)} = q_i \frac{F(i,j)}{\varepsilon_j - \varepsilon_i} \tag{10}$$

Where q_i is the donor orbital occupancy, ε_i and ε_j are diagonal elements, and F_{ij} is the off diagonal NBO Fock matrix element. The donor-acceptor interactions and their corresponding $E^{(2)}$ energies are shown in Table 7. As shown in Table 7, WB97X-D method gives the best values of $E^{(2)}$. For orientation A, an interaction between the free doublet (LP) of donor orbital of the oxygen atom (O 159) of AZ and the anti-binding acceptor orbital σ* (O 33-H 107) of β-CD positioned at 1.87 Å with a stabilization energy $E^{(2)}$ of

12.06/10.62 kcal mol^{-1} in the gas phase, another interaction is observed between the free doublet (LP) of donor orbital of oxygen atom (O 164) and anti-binding acceptor orbital σ * (O 44-H 117) positioned at 2.02 Å with a stabilization energy $E^{(2)}$ of 4.89/3.43kcal mol^{-1}. The same interaction was obtained between the free doublet (LP) of the donor orbital of oxygen atom (O 159) and the anti-binding acceptor orbital σ* (O 69-H 140) that was positioned at 1.91 Å. In orientation B, lower energy value of 6.68/6.21 kcal mol^{-1} was obtained compared to orientation A. Orientation A is strongly stabilized by the formation of hydrogen. Intermolecular hydrogen bonds exist in the geometrical structures of both orientations (Fig. 7).

From the results of NBO calculations, we can confirm that the intermolecular hydrogen interactions and charge transfer between occupied and unoccupied orbitals of host/ guest have major contribution to the stabilization of the complex.

^{1}H NMR Analysis

^{1}H NMR spectroscopy is one of the most useful techniques for studying host-guest systems, as it provides very interesting microscopic information about the structure
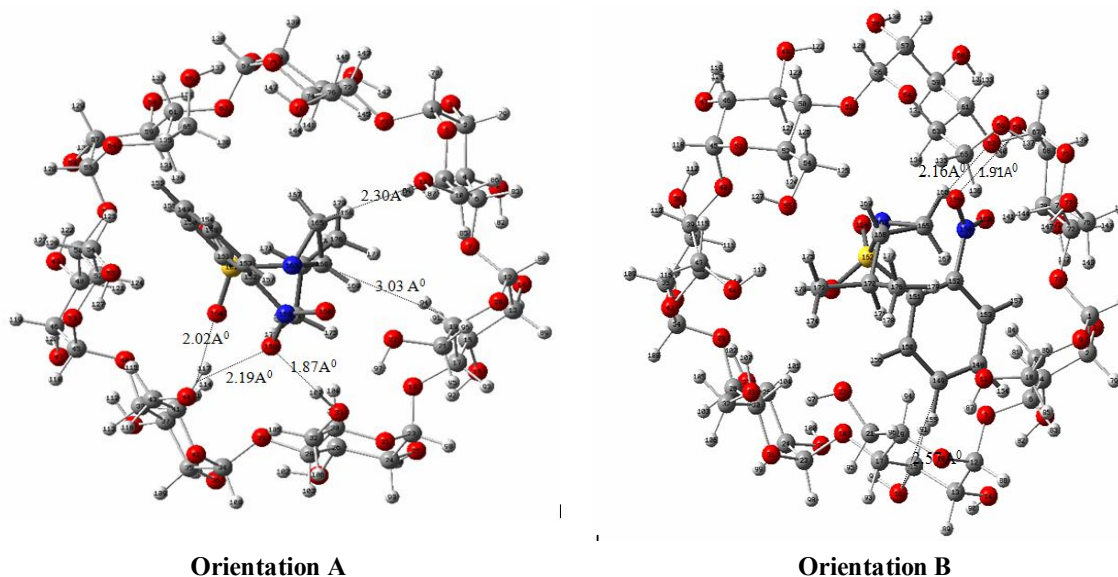
Orientation A   **Orientation B**

Fig. 7. Geometric structures of the tow orientations of the AZ/β-CD complex optimized by the NBO method, WB97X-D/6-31G(d) (a, b) in the gas phase.

of the formed molecule and the orientation of the embedded guest molecule. To better explore the introducing guest particles into the lumen of the host molecule, we calculated the chemical shifts δ. In this part, variability in H NMR chemical transitions was studied using the Gauge-Including Atomic Orbital (GIAO) approach [43]. The B3LYP/6-31G(d) method was applied using single-point calculations on geometries optimized by WB97X-D/6-31G(d) and B97D3/6-31G(d). The method was found suitable for the theoretical Proton NMR spectroscopy of organic molecules [44,45]. NMR chemical shifts (δ) were calculated by subtracting the nuclear magnetic shielding tensors of protons in molecules of interest from those in tetramethyl silane (TMS) as a reference. Chemical shift (δ) was calculated by the equation:

$$\delta = \sigma TMS - \sigma \tag{11}$$

Changes in the chemical shifts of the isolated AZ guests and their inclusion complexes are shown in Table 8 and Fig. 8.

The inclusion of AZ in the β-CD cavities was evidenced by the change in the chemical shifts of the last encapsulated protons with respect to the chemical shifts of the same protons in the free form. The values of the calculated and
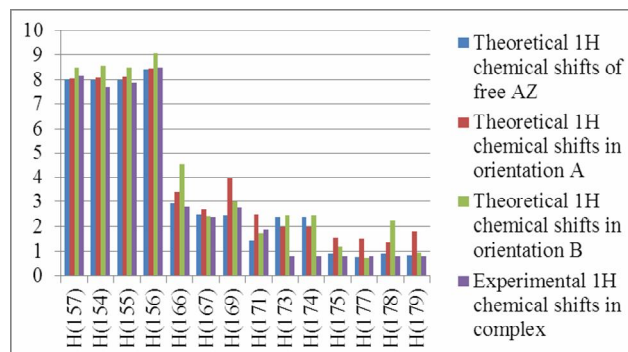
Fig. 8. Chemical shifts experimental [10] and calculated of free AZ protons and inclusion complexes AZ/β-CD by the GIAO approach, B3LYP/6-31G(d).

experimental chemical shifts [10] (H 166: 2.80 ppm), before and after the complexation, are close in orientation A (H 166: 3.42 ppm). The difference in most values does not exceed 1ppm from orientation B (δ H 166: 4.55 ppm). The largest difference between theoretical chemical transformations and experimental chemical transformations in proton (H 156: 9.04 ppm) was observed for direction B. It should be noted that the two theoretical structures presenting minimum energy are in both orientations, but on

Table 8. ^{1}H NMR Chemical Shifts (ppm) of AZ before and after Complexation Calculated by GIAO Method at B3LYP/6-31G(d) Optimized with WB97X-D/6-31g(d) and B97D3/6-31G(d) in the Aqueous Phase

Protons	Calculated			Experimental	
	AZ free	AZ in complex Orientation A	AZ incomplexe Orientation B	AZ free	AZ in complex
H(157)	8.04/0.85	8.07/8.20	8.50/8.71	8.52	8.17
H(15 4)	7.99/8.18	8.08/8.24	8.58/8.72	8.14	7.71
H(155)	7.99/8.17	8.13/8.28	8.49/8.75	8.02	7.90
H(156)	8.42/8.54	8.48/8.50	9.04/8.87	7.68	8.50
H(166)	2.93/3.10	3.42/3.18	4.55/4.41	1.50	2.80
H(167)	2.50/2.61	2.70/2.86	2.40/2.60	1.50	2.38
H(169)	2.46/2.58	3.95/3.94	2.99/2.86	1.59	2.75
H(171)	1.47/1.70	2.50/2.66	1.74/1.77	1,98	1.87
H(173)	2.38/2.47	1.98/2.24	2.44/2.56	0.88	0.82
H(17 4)	1.05/1.21	1.36/1.56	2.15/2.04	0.88	0.82
H(17 5)	0.90/1.05	1.57/1.48	1.19/1.30	0.88	0.82
H(177)	0.78/0.94	1.51/1.45	0.74/1.00	0.84	0.82
H(178)	0.92/1.08	1.36/1.56	2.21/1.98	0.84	0.82
H(179)	0.85/0.98	1.80/1.79	0.96/1.11	0.84	0.82

the basis of our theoretical results, the orientation A can be considered as the most convenient structure.

Non-covalent Interaction Analysis (NCI)

The non-covalent interaction analysis method provides a graphic visualization of regions in which non-covalent interactions such as hydrogen bonds, van der Waals interactions, and repulsive steric interactions [46,47] produce in real space. Recently, the NCI analysis has been used to identify the weak interactions from the AIM analysis [48,49]. In the 3D spatial visualization of NCI isosurface shown in Fig. 9, the color-coding scheme is as follows: Van der Waals interactions are indicated by a green spot, strong hydrogen bond interactions are represented by a blue spot, and the repulsive steric forces are visualized by the red spot. From the NCI isosurface (Fig. 9), we observed green spots between AZ and β-CD in the orientations A and B, indicating weak attraction due to the van der Waals interaction. We also observed some blue spots for hydrogen bond interactions between guest and host. There was also

the appearance of weak van der Waals, and weak intra-molecular hydrogen bond interactions in β-CD, between the primary and secondary hydroxyls, and steric repulsions in the aromatic rings of AZ and β-CD.

CONCLUSIONS

This theoretical work explored the detailed study of the inclusion complex of AZ/β-CD. The DFT functionals B3LYP, WB97X-D, and B97D3, and 6-31G(d) basis set were used in both gas and aqueous phases. Orientation A was more preferable than orientation B in both the gas and aqueous phases, which is in good agreement with the experimental results. The best results were obtained using WB97X-D and B97D3/6-31G(d). Geometry optimization calculations for the complex in the aqueous phase were almost similar to those in the gas phase. The analysis of the thermodynamic calculations indicated the negative valued for ΔG, ΔH, and ΔS, suggesting that the formation of AZ/β-CD inclusion complexes in vacuo is a spontaneous and

Orientation A   Orientation B

$\rho > 0$ sign(λ_2) ρ decrease $\rho \approx 0$ sign(λ_2) ρ increase $\rho > 0$
$\lambda_2 < 0$ ⟵ $\lambda_2 \approx 0$ ⟶ $\lambda_2 < 0$

Strong attraction: Van der Waals interaction   Strong repulsion:
H-bond, halogen-bond   Steric effect in ring and cage

Fig. 9. NCI isosurfaces for the AZ/β-CD inclusion complex calculated by method WB97X-D/6-31G(d) in gas phase.

enthalpy-driven process. The charge distribution calculated using NBO method indicated that when the guest molecule interacts with β-CD, its charge distribution changes. The NBO and NCI analysis showed that the driving forces for the formation of complexes were formation of intermolecular hydrogen bonds. Finally, the results of the RMN and GIAO calculations were in agreement with experiment.

REFERENCES

[1] Szejtli, J., Introduction and general overview of cyclodextrin chemistry. *Chem. Rev.* **1998**, *98*, 1743-1754, DOI: 10.1021/cr970022c.

[2] Szejtli, J., Past, present and futute of cyclodextrin research. *Pure Appl. Chem.* **2004**, *76*, 1825-1845, DOI: 10.1351/pac200476101825.

[3] Keniche, A.; Mezrai, A.; Mulengi, J., Synthesis of a novel class of phosphono aziridines as interesting antibacterial agents. *In: The Open Conference Proceedings Journal.* **2011**, *2*, 28-35, DOI: 10.2174/2210289201102010028.

[4] Kurmich, D.; Regan, J. R.; Disalvo, D., PCT Int. Appl., **2009**. WO 2009015067 A2 20090129. US20100048950. Application Number: 12/521005/ Publication: 02/25/2010.

[5] Kim, K.; Jordan, K. D., Comparison of density functional and MP2 calculations on the water Monomer and dimer. *J. Phys. Chem.* 1994, *98*, 10089-10094, DOI: 10.1021/j100091a024.

[6] Stephens, P. J.; Devlin, F. J.; Chabalowski, C. F.; Frisch, M. J., *Ab initio* calculation of vibrational absorption and circular dichroism spectra using density functional force fields. *J. Phys. Chem.* **1994**, *98*, 11623-11627, DOI: 10.1021/j100096a001.

[7] Head-Gordon, C., Long-range corrected hybrid density functional with damped atom-atom dispersion corrections. *J. Phys. Chem. Chem. Phys.* **2008**, *10*, 6615-6620, DOI: 10.1039/b810189b.

[8] Grimme, S.; Ehrlich, S.; Goerick, L., Effect of the damping function in dispersion corrected density functional theory. *J. Comput. Chem.* **2011**, *32*, 1456-

1465, DOI: 10.1002/jcc.21759.

[9] Becke, A. D., Density-functional thermochemistry. V. Systematic optimization of exchange-correlation functionals. *J. Chem. Phys.* **1997**, *107*, 8554-8560, DOI: 10.1063/1.475007.

[10] Keniche, A.; Slimani, M. Z.; Miranda, J. I.; Aizpurua, J. M., NMR investigation of the complexation of (S)-2-isopropyl-1-(*o*-nitrophenyl)sulfonyl)aziridine with β-cyclodextrin. *Mediterr. J. Chem.* **2014**, *2*, 620-631, DOI: 10.13171/mjc.2.5.2013.01.12.23.

[11] Frisch, M.; Trucks, J. G. W.; Schlegel, H. B.; Scuseria, G. E.; Robb, M. A.; Cheeseman, J. R., *et al.* Gaussian 09, Revision C.01; Gaussian Inc.: Wallingford, CT, USA, **2010**.

[12] James, J. P., Stewart, Stewart Computational Chemistry, Colorado Springs, MOPAC2016, CO, USA.

[13] Bolton, E. E.; Wang, Y.; Thiessen, P. A.; Bryant, S. H.; Wheeler, R. A.; Spellmeyer, D. C., Integrated platform of small molecules and biological activities. *Annual Reports in Computational Chemistry, 4, Elsevier.* **2008**, *4*, 217-241, DOI: 10.1016/S1574-1400(08)00012-1.

[14] Chem-Office 3D Ultra, Version 10 Cambridge Software **2006**.

[15] Hyperchem, Relaese 7.51 for Windows **2002** Hypercub. Inc.

[16] Stewart, J. J. P., Optimization of parameters for semiempirical methods I. *Method. J. Comput. Chem.* **1989**, *10*, 209- 220, DOI: org/10.1002/jcc.540100208.

[17] Roy, D.; Dennington, I. I.; Todd, A.; Keith etJohn, M., Millam. Gauss view 5.0, Revision C.01; Gaussian Inc.: Wallingford, CT 0642, USA, **2010**.

[18] Liu, L.; Guo, Q. X., Use of quantum chemical methods to study cyclodextrin chemistry. *J. Incl. Phenom. Macrocycl. Chem.* **2004**, *50*, 95-103, DOI: 10.1007/s10847-003-8847-3.

[19] De Sousa, S. M. R.; Guimarães, L.; Ferrari, J. L.; De Almeida, W. B.; Nascimento Jr, C. S., A DFT investigation on the host/guest inclusion process of prilocaine into β-cyclodextrin. *Chem. Phys.* **2016**, *652*, 123-129, DOI: org/10.1016/j.cplett.2016.04.053.

[20] Rahim, M.; Madi, F.; Nouar, L.; Bouhadibaa, A. E.; Haiahem, S.; Khatmi, D. E.; Belhocine, Y., Driving forces and electronic structure in β-cyclodextrin/3,3′-diaminodiphenylsulphone complex. *J. Mol. Liq.* **2014**,

199, 501-510, DOI: org/10.1016/j.molliq.2014.09.035.

[21] Djilani, I.; Madi, F.; Nouar, L.; Haiahe, M. S.; Rahim, M.; Khatmi, D. E.; Bouhadiba, A., Theoretical investigation to characterize the inclusion complex of α-lipoic acid and β-cyclodextrin. *C. R. Chim.* **2015**, *18*, 170-177, DOI: org/10.1016/j.crci.2014.05.003.

[22] Guendouzi, A.; Mekelleche, S. M.; Brahim, H.; Litim, K., Quantitative conformational stability host-guest complex of carvacrol and thymol with β-cyclodextrin: a theoretical investigation. *J. Incl. Phenom. Macrocycl. Chem.* **2017**, *89*, 143-155, DOI: org/10.1007/s10847-017-0740-6.

[23] Nouar, L.; Haiahem, S.; Abdelaziz, B.; Fatiha, M., Theoretical study of inclusion complexation of 3-amino-5-nitrobenzisothiazole with β-cyclodextrin. *J. Mol. Liq.* **2011**, *160*, 8-13, DOI: /10.1016/j.molliq.2011.02.016.

[24] Bouhadiba, A.; Belhocine, Y.; Rahim, M.; Djilani, I.; Nouar, L.; Khatmi, D. E., Host-guest interaction between tyrosine and β-cyclodextrin: Molecular modeling and nuclear studies. *J. Mol. Liq.* **2017**, *233*, 358-363, DOI: org/10.1016/j.molliq.2017.03.029.

[25] Himri, S.; Lafifi, I.; Guendouzi, A.; Cheriet, M.; Nouar, L.; Madi, F., Density functional theories study of the interactions between host β-cyclodextrin and guest 8-Anilinonaphthalene-1-sulfonate: Molecular structure, HOMO, LUMO, NBO, QTAIM and NMR analyses. *J. Mol. Liq.* **2019**, *280*, 218-229, DOI: org/10.1016/j.molliq.2019.01.019.

[26] Nouar, L.; Haiahem, S.; Abdelaziz, B.; Fatiha, M., Molecular modeling investigation of *para*-nitrobenzoic acid interaction in β-cyclodextrin. *Mol. Liq.* **2011**, *160*, 1-7, DOI: org/10.1016/j.molliq.2011.02.004.

[27] Van Duijneveldt, F. B., *et al.*, State of the art in counterpoise theory .*Chem. Rev.* **1994**, *94*, 1873-1885, DOI: org/10.1021/cr00031a007.

[28] Boys, S. F.; Bernardi, F., The calculation of small molecular interactions by the differences of separate total energies. Some procedures with reduced errors. *Mol. Phys.* **1970**, *19*, 553-566, DOI: org/10.1080/00268977000101561.

[29] Haiahem, S.; Nouar, L.; Djilani, I.; Bouhadiba, A.; Madi, F.; Khatmi, D. E., Host-guest inclusion complex between β-cyclodextrin and paeonol: A theoretical

approach. *C. R. Chim.* **2013**, *16*, 372-379, DOI: org/10.1016/j.crci.2012.11.008.

[30] SenthilRaj, P.; Periandy, S.; Xavier, S.; Attia, M. I., Molecular structure, vibrational spectra, HOMO, LUMO and NMR studies of methylphenylcyclo-propenone based on density functional theories. In: Ebenezar, J. (Ed.), Recent Trends in Materials Science and Applications. *Springer, Cham.* **2017**, *189*, 655-683. DOI: org/10.1007/978-3-319-44890-9_55.

[31] Gümüş, H. P.; Tamer, Ö.; Avcı, D.; Atalay, Y., Quantum chemical calculations on the geometrical, conformational, spectroscopic and nonlinear optical parameters of 5-(2-chloroethyl)-2,4-dichloro-6-methylpyrimidine. *Spectrochim. Acta Part A.* **2014**, *129*, 219-226, DOI: org/10.1016/j.saa.2014.03.031.

[32] Gümüş, H. P.; Tamer, Ö.; Avcı , D.; Atalay, Y., Effects of donor-acceptor groups on the structural and electronic properties of4-(methoxymethyl)-6-methyl-5-nitro-2-oxo-1,2-dihydropyridine-3-carbonitrile. *Spectrochim. Acta Part A.* **2014**, *132*, 183-190, DOI: 10.1016/j.saa.2014.04.128.

[33] Venkataramanan, N. S.; Suvitha, A.; Kawazoe, Y., Unraveling the binding nature of hexane with quinone functionalized pillar [5] quinone: A computational study. *J. Incl. Phenom. Macro.* **2019**, *95*, 307-319, DOI: org/10.1007/s10847-019-00945-3.

[34] Ramalingam, S.; Periandy, S.; Karabacak, M.; Karthikeyan, N., Spectroscopic (FT-IR/FTRaman) and computational (HF/DFT) investigation and HOMO/LUMO/MEP analysis on 2-amino-4-chlorophenol. *Spectrochim. Acta A.* **2013**, *104*, 337-351, DOI: org/10.1016/j.saa.2012.11.107.

[35] Karelson, M.; Lobanov, V. S; Katrizky, R., Quantum-chemical descriptors in QSAR/QSPR studies. *Chem. Rev.* **1996**, *96*, 1027-1044, DOI:10.1021/cr950202r.

[36] De Almeida, M. V.; *et al.,* Experimental and theoretical investigation of epoxide quebrachitol derivatives through spectroscopic analysis. *Org. Lett.* **2010**, *12*, 5458-5461, DOI: org/10.1021/ol102305x.

[37] De Almeida, M. V.; *et al.,* ^{1}H NMR analysis of *O*-methyl-inositol isomers: A joint experimental and theoretical study. *Magn. Reson. Chem.* **2012**, *50*, 608-614. DOI: org/10.1002/mrc.3848.

[38] Reed, A. E.; Weinstock, R. B; Weinhold, F., Natural atomic orbitals and natural population analysis, *J. Chem. Phys.* **1985**, *83*, 735-746, doi.org/10.1063/1.449486.

[39] Parr, R. G.; Pearson, R. G., Absolute hardness: companion parameter to absolute electronegativity, *J. Am. Chem. Soc.* **1983**, *105*, 7512-7516, DOI: org/10.1021/ja00364a005

[40] Parr, R. G.; Donnelly, R. A.; Levy, M.; Palke, W. E., Electronegativity, the density functional viewpoint. *J. Chem. Phys.* **1978**, *68*, 3801-3807, DOI: org/10.1063/1.436185.

[41] Liu, L.; Song, K. S.; Li, X. S.; Guo, Q. X., Charge-transfer interaction: A driving force for cyclodextrin inclusion complexation. *J. Incl. Phenom. Macrocycl. Chem.* **2001**, *40*, 35-39, DOI: org/10.1023/A:1011170026406.

[42] Abdelmalek, L.; Madi, F.; Nouar, L.; Cherait, M.; Merabet, N.; Khatmi, D. E., Computational study of inclusion complex formation between carvacrol and β-cyclodextrin *in vacuum* and in water: Charge transfer, electronic transitions and NBO analysis. *J. Mol. Liq.* **2016**, *224*, 62-71, DOI: org/10.1016/j.molliq.2016.09.053.

[43] Zaboli, M.; Raissi, H., The analysis of electronic structures, adsorption properties, NBO, QTAIM and NMR parameters of the adsorbed hydrogen sulfide on various sites of the outer surface of aluminum phosphide nanotube: A DFT study. *Struct. Chem.* **2015**, *26*, 1059-1075, DOI: org/10.1007/s11224-015-0563-2.

[44] Erdogdu, Y.; Manimaran, D.; Güllüolu, M. T.; Amalanathan, M.; Hubert Joe, I.; Yurdakul, S., FT-IR, FT-Raman NMR Spectra and DFT Simulations of 4-(4-fluoro phenyl)-1H-imidazole1. *Optics Spectrosc.* **2013**, *114*, 525-536, DOI: org/10.1134/S0030400X13040073.

[45] Yüksek, H.; Cakmak, I.; Sadi, S.; Alkan, M.; Baykara, H., Synthesis and GIAO NMR calculations for some novel4-heteroarylidenamino-4,5-dihydro-1*H*-1,2,4-triazol-5-one derivatives: Comparison of theoretical and experimental ^{1}H and [13]C- chemical shifts. *Int. J. Mol. Sci.* **2005**, *6*, 219-229 DOI: org/10.3390/i6060219.

[46] Zahedi, E.; Shaabani, S.; Shiroudi, A., Following the molecular mechanism of decarbonylation of unsaturated cyclic ketones using bonding evolution theory coupled with NCI analysis. *J. Phys Chem. A.*

2017, *121*, 8504-8517, DOI: org/10.1021/acs.jpca.7b08503.

[47] Venkataramanan, N. S.; Suvitha, A.; Kawazoe, Y., Density functional theory study on the dihydrogen bond cooperativity in the growth behavior of dimethyl sulfoxide clusters. *J. Mol. Liq*. **2018**, *49*, 454-462, DOI: org/10.1016/j.molliq.2017.11.062.

[48] Venkataramanan, N. S.; Suvitha, A., Nature of bonding and cooperativity in linear DMSO clusters: A DFT, AIM and NCI analysis. *J. Mol. Graph Model*.**2018**, *81*, 50-59, DOI: org/10.1016/j.jmgm.2018.02.010.

[49] Venkataramanan, N. S.; Suvitha, A.; Kawazoe, Y., Intermolecular interactions in nucleobases and dimethyl sulfoxide/water molecules: A DFT, NBO, AIM and NCI analysis. *J. Mol. Graph. Model.* **2017**, *78*, 48-60, DOI: org/10.1016/j.jmgm.2017.09.022.